UNIVERSITY OF READING

School of Mathematical and Physical Sciences

Wave Reflection and trapping in a two dimensional duct

Tahnia Appasawmy

August 2010

Supervisors:
Dr. Nick Biggs & Dr. Peter Chamberlain

This dissertation is submitted to the Department of Mathematics in partial fulfilment of the requirements for the degree of Master of Science

Abstract

Trapped modes occur in many areas in physics, we will be investigating their existence in an acoustic waveguide using Dirichlet and Neumann boundary conditions. We choose to nd these trapped modes through a perturbation method and numerically solve the problem. Further investigations will deal with the geometric structure of the waveguide and discuss the existence of these modes in various situations.

I would like to thank, both my supervisors Nick Biggs and Peter Chamberlain for their time, patience and encouragement throughout this experience. It has been more than appreciated!

List of Figures

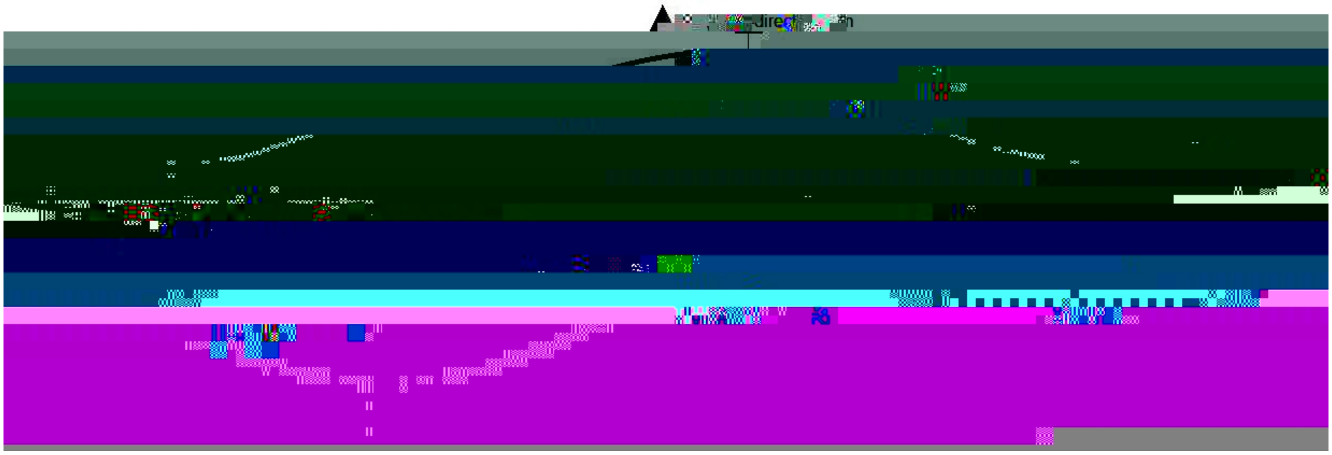

Figure 1: The waves propagating in the waveguide.

Our rst step is to non-dimensionalise the variables using the scaled equations below

$$x = \ x{=}h_0; \tag{4}$$

$$y = y{=}h_0; \tag{5}$$

$$k = kh_0; \tag{6}$$

$$(x;y) = \ (x;y); \tag{7}$$

and

$$h\ \ (x) = \frac{h\ \ (x)}{h_0}; \tag{8}$$

for some positive h_0, and h h_0

non dimensionalise in the following way:

$$\bar{x} = {}_x x_{\bar{x}} = \frac{}{h_0} \, {}_x \qquad \text{thus} \quad {}_{\bar{x}\bar{x}} = (\frac{}{h_0})^2 \, {}_{xx} \tag{10}$$

Similarly the second term non-dimensionalises as

$${}_{\bar{y}\bar{y}} = \frac{{}_{yy}}{h_0^2} \tag{11}$$

This leads to the assembled equation

$$(\frac{}{h_0})^2 \, {}_{xx} + \frac{{}_{yy}}{h_0^2} + (\frac{k}{h_0})^2 \, = 0 \tag{12}$$

This then simplifies to

$${}^2 \, {}_{xx} + {}_{yy} + k^2 \, = 0, \tag{13}$$

together with the non-dimensionalised boundary conditions

$$= 0 \qquad (\infty < x < \infty, y = h(x)), \tag{14}$$

$$\to 0 \qquad \text{as } x \to \infty. \tag{15}$$

2.2 Perturbation method

We are now able to construct an asymptotic expansion in powers of the small parameter using a perturbation method closely related to the WKBJ theory. The method is an approximation to the characteristics of the waves in a slowly varying waveguide. The wave function (x, y) can be written as an exponential of another function , such that

$$= A(x, y)e^{(P(x,y))}, \tag{16}$$

where

$$A = A_0(x, y) + A_1(x, y) + {}^2 A_2(x, y) + \ldots \tag{17}$$

and

$$P = {}^1 P_1(x, y) + P_1(x, y) + {}^2 P_2(x, y) + \ldots \tag{18}$$

From above, A_0 represents the adiabatic approximation, meaning the system remains in its instantaneous eigenstate whilst a perturbation is implemented, the higher orders correspond to the amplitude terms along the transverse wave field. P is the phase of the wave expanded in terms of , it must be complex valued, as to ensure the WKBJ asnsatz (16) includes all cases

of wave activity, ie propagating and decay. Note we can ignore an $O(\ ^0)$ term from equation (18) since it can be accounted for by the rst term in equation (17).We now substitute the ansatz into (13) in the following way:
Using equation(17), we see that

$$
\begin{aligned}
{}_x(x;y) &= AP_x e^P + A_x e^P; && (19)\\
\text{and} \quad {}_{xx}(x;y) &= AP_x^2 e^P + (AP_{xx} + P_x A_x)e^P + A_x P_x e^P + A_{xx} e^P; && (20)
\end{aligned}
$$

and similarly

$$
{}_{yy}(x;y) = AP_y^2 e^P + (AP_{yy} + P_y A_y)e^P + A_y P_y e^P + A_{yy} e^P: \qquad (21)
$$

We now substitute (20), (21) and (16) into the Helmholtz equation and expand to obtain

$$
{}^2[AP_x^2 e^P + (AP_{xx} + P_x A_x)e^P + A_x P_x e^P + A_{xx} e^P]+
$$

$$
[AP_y^2 e^P + (AP_{yy} + P_y A + y)e^P + A_y P_y e^P + A_{yy} e^P] + [k^2 A e^P] = 0
$$

Cancelling a factor of e^P then gives

$$
{}^2[AP_x^2 + (AP_{xx} + P_x A_x) + A_x P_x + A_{xx}] + [AP_y^2 + (AP_{yy} + P_y A + y) + A_y P_y + A_{yy}] + k^2 A = 0: \qquad (22)
$$

Now substituting(17) and (18) into(22) and expand for small , we nd that.

$$^{2}[(A_0 + A_1 + {}^{2}A_2 + :::)({}^{2}P^{2}{}_{1x} + 2P {}_{1x}P_{1x} + P_{2x} + {}^{2}P_{1x}^{2} + {}^{3}P_{1x}P_{2x} + :::)]$$

$$+(A_0 + A_1 + {}^{2}A_2 + :::)({}^{1}P {}_{1xx} + {}_{1}P_{1xx} + {}^{2}P_{2xx} + :::)$$

$$+2[(A_{0_x} + A_{1_x} + {}^{2}A_{2_x} + :::)({}^{1}P {}_{1_x} + {}_{1}P_{1_x} + {}^{2}P_{2_x} + :::) + (A_{0_{xx}} + A_{1_{xx}} + {}^{2}A_{2_{xx}} + :::)]$$

$$+[(A_0 + A_1 + {}^{2}A_2 + :::)({}^{2}P^{2}{}_{1y} + 2P {}_{1y}P_{1y} + P_{2y} + {}^{2}P_{1y}^{2} + {}^{3}P_{1y}P_{2y}:::)]$$

$$+(A_0 + A_1 + {}^{2}A_2 + :::)(+ P$$

$$A_{0_{yy}} + A_0(f'^2 + k^2) = 0$$

which is a second order differential equation with solution

$$A_0 = C_1 \cos(y\lambda(x)) + C_2 \sin(y\lambda(x)); \tag{25}$$

where $\lambda^2(x) = f'^2 + k^2$ and $C_1 = C_1(x); C_2 = C_2(x)$. Using the Dirichlet conditions, the solution is

$$A_0 = C_3 \sin((y + h_-)\lambda(x)); \tag{26}$$

for $C_3 = C_3(x)$. Then either $C_3 = 0$ leading to a trivial solution or $\lambda(x)(h_+ + h_-) = n\pi$. We have $A_0 = a_0(x)S(x; y)$ where $S(x; y) = C_3 \sin(\lambda(x)(h_+ + h_-))$, and $\lambda_n(x) = \frac{n\pi}{w(x)}$ for repeated solutions of the sin function, $n = 1; 2 :::$, $w(x) = [h_+(x) + h_-(x)]$ and $a_0(x)$, is a function of x we later calculate. Firstly, we normalise the function of $S(x; y)$ in order to find the value for C_3.

$$\int_{-h_-}^{h_+} C_3^2 \sin^2(\lambda(x)y + h_-)\, dy = 1 \tag{27}$$

Using a trigonometric identity, we separate the terms,

$$\int_{-h_-}^{h_+} \frac{C_3^2}{2} - \frac{C_3^2}{4n\pi} \sin\frac{(2n\pi(y + h_-))}{w(x)}\, dy = 1 \tag{28}$$

integrating and evaluating at the limits, the equation is thus

$$C_3^2(h_+(x) + h_-(x)) = 2 \tag{29}$$

rearranging appropriately we see

$$C_3 = \left(\frac{2}{(h_+(x) + h_-(x))}\right)^{\frac{1}{2}}: \tag{30}$$

Therefore

$$S(x; y) = \left(\frac{2}{(h_+(x) + h_-(x))}\right)^{\frac{1}{2}} \sin(\lambda(x)(y + h_-)) \tag{31}$$

We continue equating orders of ϵ. The $O(\epsilon^1)$ terms are

$$A_1 P^2_{1x} + A_0 P_{-1xx} + 2A_{0x}P_{-1x} + 2P_{1y}P_{1y}A_1 + A_0 P_{2y} + A_0 P_{1yy} + 2A_{0y}P1_y + A_{1yy} + k^2 A_1 = 0$$

Recalling that $P_{-1} = f(x)$ and the derivatives of this function, we implement this in the equation above

$$A_{1yy} + A_1 P^2 \;{}_{1x} + k^2 + A_0(f_n'' + P_{1yy}) + 2A_{0x}f'_n + 2A_{0y}P_{1y}; = 0$$

$$\text{ie.} A_{1yy} + A_1(P^2{}_{1x} + k^2) = \quad A_0(f_n'' + P_{1yy}) \quad 2A_{0x}f'_n \quad 2A_{0y}P_{1y}. \tag{32}$$

Now multiply (32) by A_0 and integrate from $y = \quad h \quad$ to $y = h_+$ which leads to

$$\int_{h}^{h_+} [A_{1_{yy}} + \;{}^2_n A_1] A_0 \, dy = 0. \tag{33}$$

Integrating by parts, we see the integration evaluates to zero.

$$A_0 A_{1_y} \Big|_{h}^{h_+} + \left(\int_{h}^{h_+} A_{1_y} A_{0_y} \, dy + \;{}^2_n \int_{h}^{h_+} A_0 A_1 \right) dy = 0. \tag{34}$$

$$A_0 A_{1_y} \Big|_{h}^{h_+} \left(A_1 A_{0_y} \right) \Big|_{h}^{h_+} + \int_{h}^{h_+} A_{0_{yy}} A_1 \, dy + \;{}^2_n A_0 A_1 \Big|^{h_+} \quad) A_0 A_1 \Big|_{h} = 0. \tag{35}$$

Since we know the function of A_1

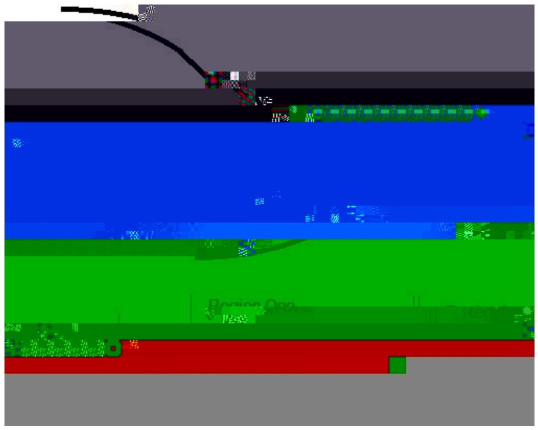

Figure 2: Diagram illustrating a tapered duct

$\int_{h}^{h_+} a_0^2 S_n^2(x;y)\,dy$ such that equation (39) reduces to

$$\frac{d}{dx}(f_n' a_0^2) = 0. \tag{40}$$

Integrating both sides we nd, $a_0(x) = C_4 |f_n'|^{\frac{1}{2}}$, for some constant C_4.

To solve for f we must rstly consider two cases for $^2(x) \quad k^2 \quad 0$ and $^2(x) \quad k^2 \quad 0$:

$$f(x) \quad f_n = \begin{cases} i \int^{x} (k^2 \quad {}_n^2(x_0))^{\frac{1}{2}}\,dx_0; & k \quad {}_n(x) \\ i \int^{x} ({}_n^2(x_0) \quad k^2)^{\frac{1}{2}}\,dx_0; & k \quad {}_n(x) \end{cases} \tag{41}$$

This de nes the two cases of the problem. When the wavenumber k is larger than the cut-o frequency ${}_n(x)$, then the trapped mode is propagating.
If however the wavenumber k

travelling wave to oscillate, passing through to the tapered region we have labelled region two. In this region the wave is evanescent and hence will exponentially decay. We find the incoming wave mostly reflecting back into region one while only a fraction of the wave transmits into the tapered region.

so that, in the limit $x_0 \to x_n^{(-)}$ there is a non-uniformity when $(x_n - x_0)^{\frac{3}{2}} = O(\ )$. Similarly for the evanescent case in the limit $x_0 \to x_n^{(+)}$, we have

$$\exp\left(-\ {}^{1} \int_{x_n}^{x} (\ {}_n^2(x_0) - k^2)^{\frac{1}{2}}\, dx_0\right) = \exp\left(-\frac{2}{3}\ {}^{1}\ {}_n^{\frac{1}{2}} (x_0 - x_n)^{\frac{3}{2}}\right); \tag{49}$$

so again there is a non-uniformity when$(x_0 - x_n)^{\frac{3}{2}} = O(\ )$. We can now utilise this knowledge in our governing equation,by setting ${}_n(x; y) = {}_n(\ )S_n(x; y)$, where $= {}^{\frac{2}{3}}(x_0 - x_n)$ is $O(1)$ in the region of interest. Now

$$_x = {}_n^{\prime}\ {}_x S_n + {}_n \frac{\partial S_n}{\partial x} = {}^{\frac{2}{3}}\ {}_n^{\prime} S_n + {}_n \frac{\partial S_n}{\partial x}. \tag{50}$$

Differentiating again we have

$$_{xx} = {}^{\frac{4}{3}}\ {}_n^{\prime\prime} S_n + 2\ {}^{\frac{2}{3}}\ {}_n^{\prime} \frac{\partial S_n}{\partial x} + {}_n \frac{\partial^2 S_n}{\partial x^2} \text{ so that} \tag{51}$$

$$^2\ {}_{xx} = {}^{\frac{2}{3}}\ {}_n^{\prime\prime} S_n + 2\ {}^{\frac{4}{3}}\ {}_n^{\prime} \frac{\partial_n S_n}{\partial x} + O(\ {}^2) \tag{52}$$

$$\text{lastly} \quad {}_{yy} = {}_n S_n\ {}_n^2(x) \tag{53}$$

since as previously stated $S_n(x; y) = (2/w)^{\frac{1}{2}} \sin[\ {}_n(y - h\ )]$. Finally the last term of the Helmholtz equation

$$k^2 = k^2\ {}_n S_n. \tag{54}$$

But $x = x_n + {}^{\frac{2}{3}}$, so $f(x) = f(x_n) + {}^{\frac{2}{3}} f'(x_n) + \frac{1}{2} {}^{\frac{4}{3}} {}^{2} f''(x_n) + O({}^{2})$
Hence equation (57)

$$ {}^{\frac{2}{3}} {}_{n}''S_n(xn;y) + {}^{\frac{2}{3}} S_{n_x}(x;y) + O({}^{\frac{4}{3}}) + 2 {}^{\frac{4}{3}}; {}_{n}' fS_{n_x}(x_n;y) + O({}^{\frac{2}{3}}g) \quad {}_{n} \quad {}_{n} {}^{\frac{2}{3}} fS_n(x_n;y) + O({}^{\frac{2}{3}})g + O({}^{2}) = 0 \tag{58}$$

We can rearrange, such that

$$ {}^{\frac{2}{3}}({}_{n}'' \quad {}_{n} \quad {}_{n})S_n = {}^{\frac{4}{3}}({}_{n}'' + 2 {}_{n}' \quad {}_{n} {}^{2} \quad {}_{n}) \frac{\partial S_n}{\partial x}(x_n) + O({}^{2}).$$

Taking the leading order ${}_{n} \quad {}_{n}^{(0)}$ where

$$ {}_{n}^{(0)''} \quad {}_{n} \quad {}_{n} = 0$$

This di erential equation is of the form of an Airy equation, and hence the solution may be written in term of the Airy functions,

$$ {}_{n}^{(0)} = F_n \mathrm{Ai}({}_{n}^{\frac{1}{3}}) + F_{2_n} \mathrm{Bi}({}_{\mathrm{n}}^{\frac{1}{3}});$$

where Ai and Bi are the Airy's function of the rst and second kind respectively and F_n and F_{2_n} are constants. Since the solution is bounded and decreases exponentially in the positive limit equation (49), then the Airy's function of the second kind is not part of the solution. Hence

$$ {}_{n}^{(0)} = F_n \mathrm{Ai}({}_{n}^{\frac{1}{3}});$$

where F_n is^2 som15 cm []6203.86 Tf 9.538 1.793 Td [(is)-326..9701 Tf 7.578 -1o(y)-326(b)-27(e)]TJ 0 -17.97

Firstly consider the limit in the negative direction:

$$_{n} \quad \frac{F_n[\exp\{i(\frac{2}{3} \quad {}_{n}^{\frac{1}{2}}(\quad)^{\frac{3}{2}} + \frac{}{4})\} \quad \exp\{\quad i(\frac{2}{3} \quad {}_{n}^{\frac{1}{2}}(\quad)^{\frac{3}{2}} + \frac{}{4})\}]}{2i \quad ^{\frac{1}{2}} \quad {}_{n}^{\frac{1}{12}}(\quad)^{\frac{1}{4}}}. \tag{62}$$

Compare with the expansion of equation (44)

$$_{n} \quad \frac{I \exp\{\quad i\frac{2}{3} \quad {}_{n}^{\frac{1}{2}}(\quad)^{\frac{3}{2}}\} + R_n \exp\{i\frac{2}{3} \quad {}_{n}^{\frac{1}{2}}(\quad)^{\frac{3}{2}}\}}{{}_{n}^{\frac{1}{2}} \quad ^{\frac{1}{2}}(\quad)^{\frac{1}{4}}}. \tag{63}$$

We see that

$$\frac{I \exp\{\quad i(\frac{2}{3} \quad {}_{n}^{\frac{1}{2}}(\quad)^{\frac{3}{2}})\}}{{}_{n}^{\frac{1}{4}} \quad ^{\frac{1}{2}}(\quad)^{\frac{1}{4}}} = \quad \frac{iF_n \exp\{\quad i(\frac{2}{3} \quad {}_{n}^{\frac{1}{2}}(\quad) + \frac{}{4})\}}{{}_{n}^{\frac{1}{12}}(\quad)^{\frac{1}{4}} 2 \quad ^{\frac{1}{2}}}; \tag{64}$$

only if

$$\frac{2^{p}\overline{} I \exp i(\frac{}{4})}{{}_{n}^{\frac{1}{6}} \quad ^{\frac{1}{6}}} = \quad iF_n. \tag{65}$$

Similarly we see that

$$\frac{R_n \exp(i\frac{2}{3} \quad {}_{n}^{\frac{1}{2}}(\quad)^{\frac{3}{2}})}{^{\frac{1}{4}}}$$

0 F28 d 26 2 6701 d 229 41 397 527 [(n)]TJ / F 5 (3) 1 5 4J 45 1 0 9552 3.59 543 4

4) 1

throughout the duct, hence we are able to construct an expansion of the form,

$$(x;y) = B(x;y)\mathrm{Ai}(\,\frac{2}{3}g(x)) + C(x;y)\mathrm{Ai}'(\,^{\frac{2}{3}}g(x)); \tag{70}$$

where

$$B = B_0 + \,^{\frac{2}{3}}B_1 + \,^{\frac{4}{3}}B_2 + ::: \tag{71}$$

$$C = \,^{\frac{2}{3}}C_1 + \,^{\frac{4}{3}}C_2 + ::: \tag{72}$$

$$g = g_0 + \,^{\frac{2}{3}}g_1 + \,^{\frac{4}{3}}g_2 + ::: \tag{73}$$

$$\tag{74}$$

The constant term in the expansion of C is not included, as we know from equation (59) the bounded solution includes only the Airy function and not the rst derivative. Now we substitute these equations into the Helmholtz equation once again, and expand to obtain

$$\begin{aligned} ^2\,_{xx} = \,& ^2B_{xx}\mathrm{Ai} + 2B_x\mathrm{Ai}'(\,^{\frac{2}{3}}g)g'\,^{\frac{4}{3}} + B\mathrm{Ai}''(\,^{\frac{2}{3}}g)g'^2\,^{\frac{8}{3}} + B\mathrm{Ai}'(\,^{\frac{2}{3}}g)g''\,^{\frac{4}{3}} \\ &+ \,^2C_{xx}\mathrm{Ai}'(\,^{\frac{2}{3}}g) + 2C_xA''(\,^{\frac{2}{3}}g)g'\,^{4}3 + C\mathrm{Ai}'''(\,^{\frac{2}{3}}g)g'^2\,^{\frac{4}{3}} \end{aligned} \tag{75}$$

$$_{yy} = B_{yy}\mathrm{Ai}(\,^{\frac{2}{3}}g(x)) + C_{yy}\mathrm{Ai}'(\,^{\frac{2}{3}g(x)}) \tag{76}$$

$$k$$

Now we equate coe cients of each power of to zero. The $O(^{(0)})$ terms are

$$
\begin{aligned}
g_0 g_0'^2 B_0 + k^2 B_0 + B_{0_{yy}} &= 0 \\
B_{0_{yy}} + B_0(k^2 + g_0 g_0'^2) &= 0 \qquad (80)
\end{aligned}
$$

Let $^2_n(x) = (k^2 + g_0 g_0^{2'})$, such that we have a simpli ed second order di erential equation, very similar to the expression 25, we can deduce g_0 is related to function f_n

$$B_{0_{yy}} + B_0(^2) = 0. \qquad (81)$$

The general solution

$$B_0 = b_1 \cos(_n(x)y) + b_2 \sin(_n(x)y) \qquad (82)$$

Using the Dirichlete(82)

such that the solution takes the form,

$$g_0(x) = \begin{cases} (\frac{3}{2}\int^{x}(k^2 \quad {}_n^2(x_0))^{\frac{1}{2}}\,dx_0)^{\frac{2}{3}}; & x \quad x_n \\ (\frac{3}{2}\int^{x}(\quad {}_n^2(x_0) \quad k^2)^{\frac{1}{2}}\,dx_0)^{\frac{2}{3}}; & x \quad x_n \end{cases} \tag{88}$$

Continuing the order of equating coe cients of the airys function

$$^{\frac{2}{3}} : k^2 B_1 + B_{1_{yy}} + (g_1 g_0^{0^2} + 2g_0 g_{1^0} g_{0^0})B_0 + g_0 g_0^{0^2} B_1 + g_0^2 g_0^{00} \tag{89}$$

And as before consider

$$B_{1_{yy}} + (k^2 + g_0 g_0^{2^0})B_1. \tag{90}$$

Let $k^2 + g_0 g_0^{2^0} = {}_n^2$ Multiplying equation (90) by B_0 and integrating from $y = \quad h \quad$ to $y = \quad h_+$ the solution =0. Then by this solvability condition,

$$\int_{h}^{h_+} g_0^0(g_0^0 g_1 + 2g_0 g_1^0)B_0\,dy = 0 \tag{91}$$

$$\int_{h}^{h_+} [g_0^{2^0} g_1 + 2g_0 g_0^0 g_1^0]B_0\,dy = 0 \tag{92}$$

Then di erentiating with respect to x,

$$\int_{h}^{h_+} \frac{@}{@x}(g_0 g_1^2)\,dy \tag{93}$$

We can then reduce the equation further

$$\frac{d}{dx}(g_0 g_1^2) = 0 \tag{94}$$

$0g_0$]

Solving this rst order di erential, leads to the solution $g_1 = Gjg_0j \quad \frac{1}{2}$ Therefore B_1

Once again, we expand through B and C term,

$$\frac{8}{3}C_{1_{xx}} + \frac{10}{3}C_{2_{xx}} + k^2\left(\frac{2}{3}C_1 + \frac{4}{3}C_2\right) + \left(\frac{2}{3}C_{1_{yy}} + \frac{4}{3}C_{2_{yy}}\right) +$$

$$g_0 g_0^{2'} C_1 \;{}^{\frac{2}{3}} + \frac{4}{3} g_0' B_0 + (g_{1''}B_0 + g_0' B_1)\;{}^{2} + (g_{2''}B_0 + g_{1''}B_1 + g_{0''}B_2)\;{}^{\frac{8}{3}}$$

$$+(g_{2''}B_1 + g_{1''}B_2)\;{}^{\frac{10}{3}} + 2g_{0'}B_{0'}\;{}^{\frac{4}{3}} + (2g_{2'}B_{0_x} + 2g_{2'}B_{2_x} + 2g_{0'}B_{2_x})\;{}^{\frac{8}{3}} +$$

$$(2g_{2'}B_{1_x} + 2g_{1'}B_{2_x})\;{}^{\frac{10}{3}} + [(g_1 g_{0'}^2 + 2g_0 g_{1'} g_{0'} C_1 + g_0 g_0^{2'} C_2]\;{}^{\frac{4}{3}} = 0.$$

0 0 359 0 0 3 653 0 27 5 9776 455 367 552 73 2 956 ( ) 26 7 97004 16 n67 5 26 ( ) n n

and thus

$$\frac{n}{S_n(x;y)} = \quad iG_n \ \tfrac{1}{6}[\exp i(\tfrac{}{4} + \textstyle\int_x^{x_n}$$

as the limits are now between 0 and $_n{}^{1}(k)$, where $_n{}^{1}(k)$ is the unique positive root of $_n(\ _n{}^{1}(k)) = k$ in the interval $(0; 1)$. If we now denote the m-th root of $\mathrm{Ai}(z) = 0$ by $z\ _m$ for $m\ 2\ \mathbb{N}$, such that the ordering of the roots are established as $z\ _{(m+1)}\quad z\ _m$, then approximations to wavenumbers k for the antisymmetric modes can be found by solving

$$\frac{2}{3} g_{0_n}(0; k) = z_m \text{ for m,n } 2\ \mathbb{N} \tag{117}$$

and for the symmetric case, by denoting z^0_m as the m-th root at $\mathrm{Ai}(z) = 0$ with the roots ordered $z^0\ _{(m+1)}\quad z^0\ _m$, the wavenumbers producing trapped modes are found via, the equation

$$\frac{2}{3} g_{0_n}(0; k) = z^0_m \text{ for m,n } 2\ \mathbb{N} \tag{118}$$

Having found the speci c wavenumbers to these trapped modes, we can implement the data into equation (116) in order to determine the structure of the waveguide. A Numerical solution, provides a clear graphical representation, of the results, as can be found in a later chapter of this paper.

3 The Neumann Problem

We will now consider the Neumann boundary condition, and compare the results to the Dirichlet.

$$_{xx} + \ _{yy} + k^2 \ = 0 \qquad (\ 1 < x < 1; y = \ h\ (x)); \tag{119}$$

$$_{\&} = 0; \qquad (\ 1 < x < 1; y = \ h\ (x)): \tag{120}$$

where & is the normal of the waveguide. The Neumann Case, follows a similar method to nding a solution as to the Dirichlet Problem. By non-dimensionalising the problem as before, substitute the given ansatz (16), (18) and (17), and expand the equation. Then by equating orders of we eventually get to the complementary function (25), where coe cients C_1 and C_2 are determined by the Neumann Boundary Condition (120). By di erentiating (25), we see that the particular solution is $C_n(x; y) = C_3 Cos((y + h\ )\quad (x)) = 0$. We also require, when $y = h_+$

$$A^0_0 = \ C_1 \cos(\ (h_+ + h\ )) = 0 \tag{121}$$

let $w(x) = (h_+ + h\ )$ then either $C_1 = 0$ which is trivial, or, $w = n$ for n $w = n$

$$C_n(x;y) = C_3 \cos(\frac{n}{w(x)}(y + h \;)) = 0; \tag{122}$$

for n=0,1,2,... Again, we normalise the function to nd C_3

$$C_n(x;y) = 1 \qquad \text{for } n = 0 \tag{123}$$

$$C_n(x;y) = \sqrt{\frac{2}{w(x)}} \cos[\frac{n}{w(x)}(y + h \;)] \quad \text{for } n = 1;2::: \tag{124}$$

Re ecting the waves in the small neighbourhood, $x = x_n$) we substitute $C(x;y) = C$

We see that

$$\frac{I \exp\{\ \ i(\frac{2}{3}\ \ {}_n^{\frac{1}{2}}(\ \ )^{\frac{3}{2}})\}}{{}_n^{\frac{1}{4}}\ {}^{\frac{1}{2}}(\ \ )^{\frac{1}{4}}} = \frac{iF_n \exp\{\ \ i(\frac{2}{3}\ \ {}_n^{\frac{1}{2}}(\ \ ) + \frac{}{4})\}}{{}_n^{\frac{1}{12}}(\ \ )^{\frac{1}{4}}2\ \ ^{\frac{1}{2}}}; \tag{129}$$

only if

$$iF_n = \frac{2^{p\_}I \exp\{i(\frac{}{4})\}}{{}_n^{\frac{1}{6}}\ {}^{\frac{1}{6}}}: \tag{130}$$

$$iF_n = \frac{2^{p\_}R_n \exp\{\ \ i(\frac{}{4})\}}{{}_n^{\frac{1}{6}}\ {}^{\frac{1}{6}}}; \tag{131}$$

and

$$F_n = \frac{2^{p\_}T_n}{{}_n^{\frac{1}{6}}\ {}^{\frac{1}{6}}}: \tag{132}$$

As before we can derive a uniformly valid solution using the expansion

$$(x;y) = B(x;y)\mathrm{Ai}(\ \ \frac{2}{3}g(x)) + C(x;y)\mathrm{Ai}^{0}(\ \ {}^{\frac{2}{3}}g(x)); \tag{133}$$

where $B(x;y)$,$C(x;y)$ and $g(x)$ are de ned in equations (71),(72),(73) respectively. Substituting the ansatz into equation 13 and separating the terms of the Airy's equations, and of the rst derivative of the Airy's equation. We then equate orders of . These terms, are replicated from the Dirichlet example, however the solution, varies from the sin function to the cos solution for the Neumann case. For example, in the equation (82), we use the Neumann condition instead, such that

$$B_0 = b_0(x)(b_3 \cos(\ \ {}_n(x)(y + h\ \ ))); : \tag{134}$$

Again, by normalising the function, we nd $b_3 = \sqrt{\frac{2}{w(x)}}$, so that $B_0 = \sqrt{\frac{2}{w}}$

waves within a tapered duct, bounded by a Nuemann condition, we may now consider nding trapped modes. This again, is the same method for the Dirichlet case, hence it deems unnecessary to replicate chapter 2.5.
We may now begin to look at the Numerical approximations to this problem and determine the trappings for each case.

4 The Numerical Approach

4.1 Plotting solutions of k

The speci c values of k are found by solving equations (117) and (118). Table 1 in the appendix shows a list of the rst 24 solutions of the Airy function and the rst derivative, denoted by Z_n and Z_n^0 for the antisymmetric and symetric solutions respectively. Let us consider the trapped modes for the rst antisymmetric soltuion, Z_1, the program, developed through MATLAB, predicts the rst two solutions of k using equation (118). To gain a better accuary of the solution, the program was developed, such that it included a numerical technique, similar to the Euler Method. This involved nding subsequent values for wavenumber k through the given equation and improving this result by averaging the calculated value with a predicted value formed from the tangent of the two preceeding values. This method was applied to the remaining Z_n solutions and the plotted result can be seen in gure (3).

This approach was also applied to the symmetric solutions as illustrated in gure (4). It is clear to see from gures (3) and (4), although not labelled, Z_1 (and Z_1^0) are the lowest solutions plotted on both graphs, increasing up to Z_n or Z_n^0.
The graphs illustrate the wavenumbers k, as a function of the bulge half width denoted h_1, such that $2h_1$ is the maximum of the bulge (at $x = 0$) and $h_1 = 2$ at the limits x ! 1. Fixing $= 0{:}1$ and the constant $G_n = 1$, we will compare solutions of k, for $n = 1$, where n is the multiple coe cient of , in the $_n(x)$ equation Figure (3) and (4) show the solutions of $\frac{k}{}$ tending to $0{:}5$ at the maximum of the bulge, which slowly decreases as we tend towards the cut-o frequency x ! 1. We would expect this, as this shows a decrease in existing trapped modes, in the given region.
It is important to mention that despite the improvement to the numerical technique used to get a more accurate solution at $h_1 = 1$, it was still di cult to get certain solutions of Z to a more accurate limit. This was because, at this region we were interpolating for asymptotic solutions.

We will now consider when $n = 2$, gures (5) and (6) illustrate the solutions of $\frac{k}{}$ to be closer together, the gaps between Z_n and Z_n^0 solutions are less far apart then in gures

n=1 bulge.jpg

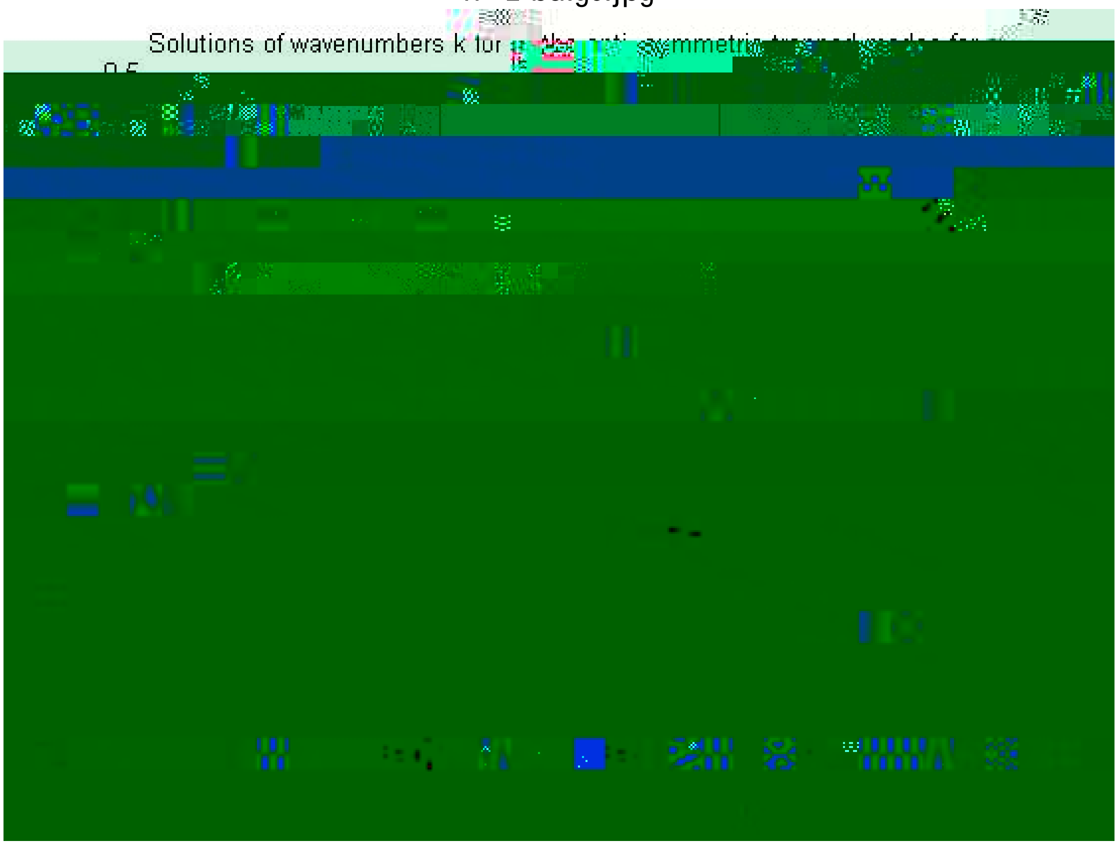

Figure 3: Solutions to wavenumbers of antisymmetric trapped modes for n=1 are plotted for each Airy solution, with the first solution Z_1 plotted as the lowest line increasing up to Z_n for n=24

n=1 bulge.jpg

Figure 4: Solution to wavenumbers of symmetric trapped modes for n=1 are plotted for each

n=2 bulge.jpg

n=2 bulge.jpg

Figure 6: Wavenumbers of symmetric trapped modes for n=2.

bulge anti-symmetric n=1.jpg

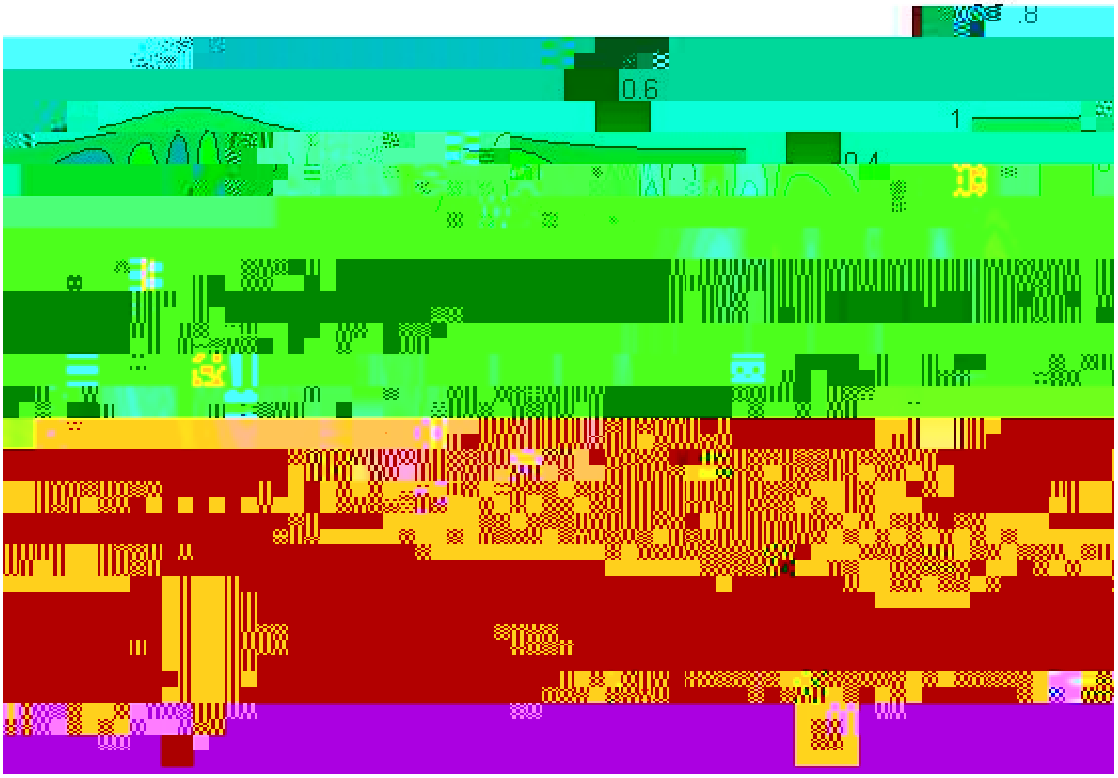

Figure 7: Contour plot of antisymmetric trapped modes.

4.2 Plotting the nal solutions with Dirichlet boundary conditions

Once the values of k were found, we substituted them into the (109) and plotted the solutions, as shown in gures (7) and (8). The graphs illustrate one trapped mode propagating at the center of the bulge. Analysing gure (8), we can see at $x = 0$ the solution is re ected such that the complete solution is symmetric. For the antisymmetric case, gure (7), involved plotting the negative solutions of $_n(x;y)$ against x and y.

A more visual representation of the trapped modes in the tapered duct can be viewed in gures (9) and (10). For the symmetric case it is very easy to see the symmetry at x=0, with large amplitudes near the cut-o frequency and small amplitudes at the centre. This suggest the resonance is at its largest at the cut-o regions, before it decays exponentially at x ! 1. The antisymmetric case is very similar, in that the resonant amplitude is at its maximum near the cut-o frequency for x incut-o i013ef 105(i010.384 -7t)-296u7t ui-s28h7hf2reisx bulge symmetric n=1.jpg

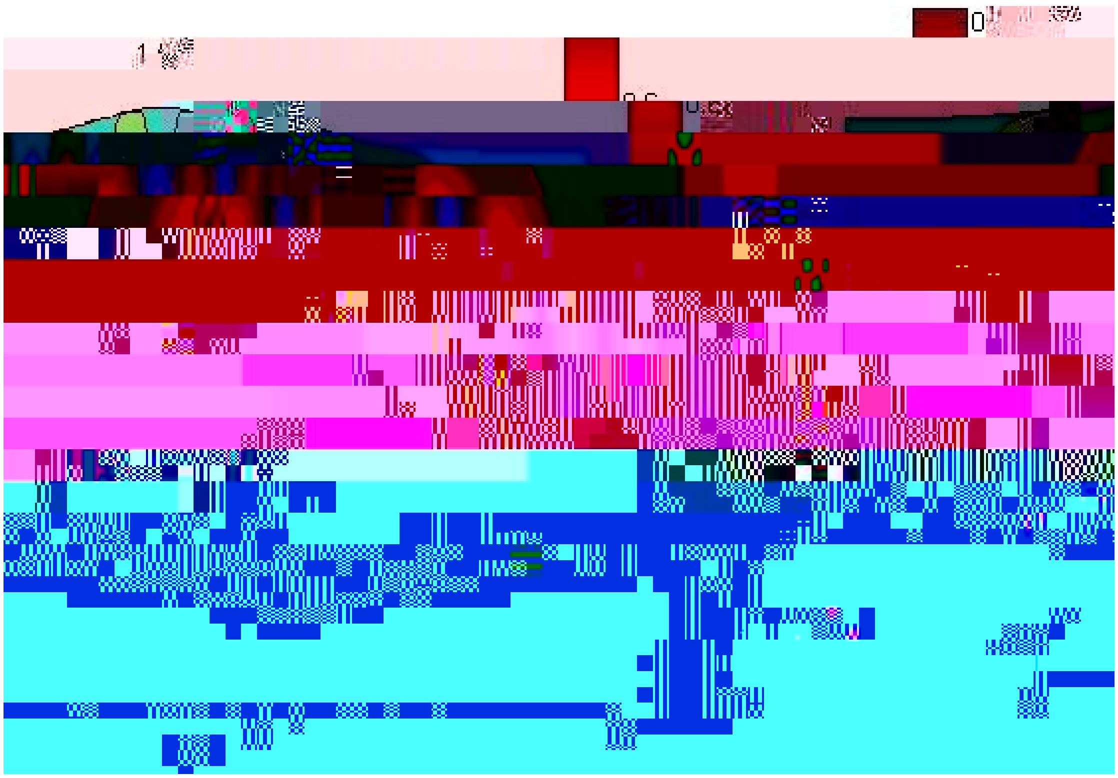

Figure 8: Contour plot of the symmetric trapped modes.

modes antisymmetric n=1.jpg

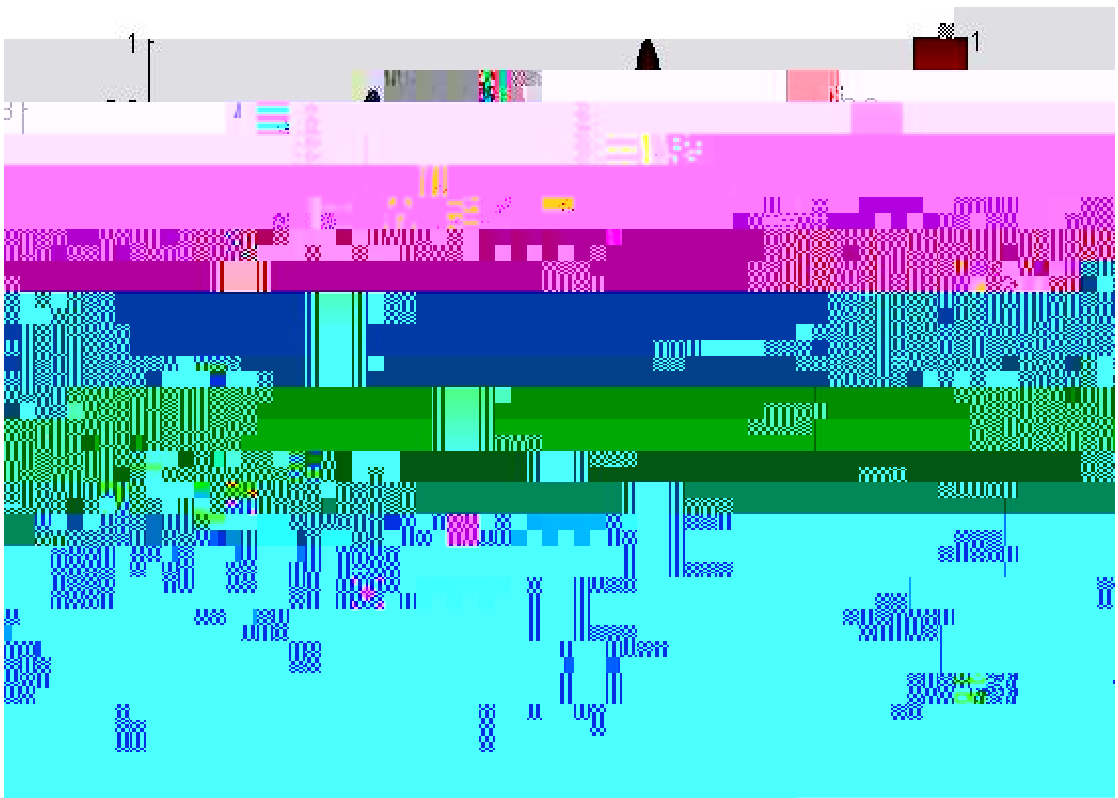

Figure 9: Surface plot of antisymmetric trapped modes, where we let $h_1 = 1{:}224$ and wavenumber $k = 1{:}500052$

modes symmetric n=1.jpg

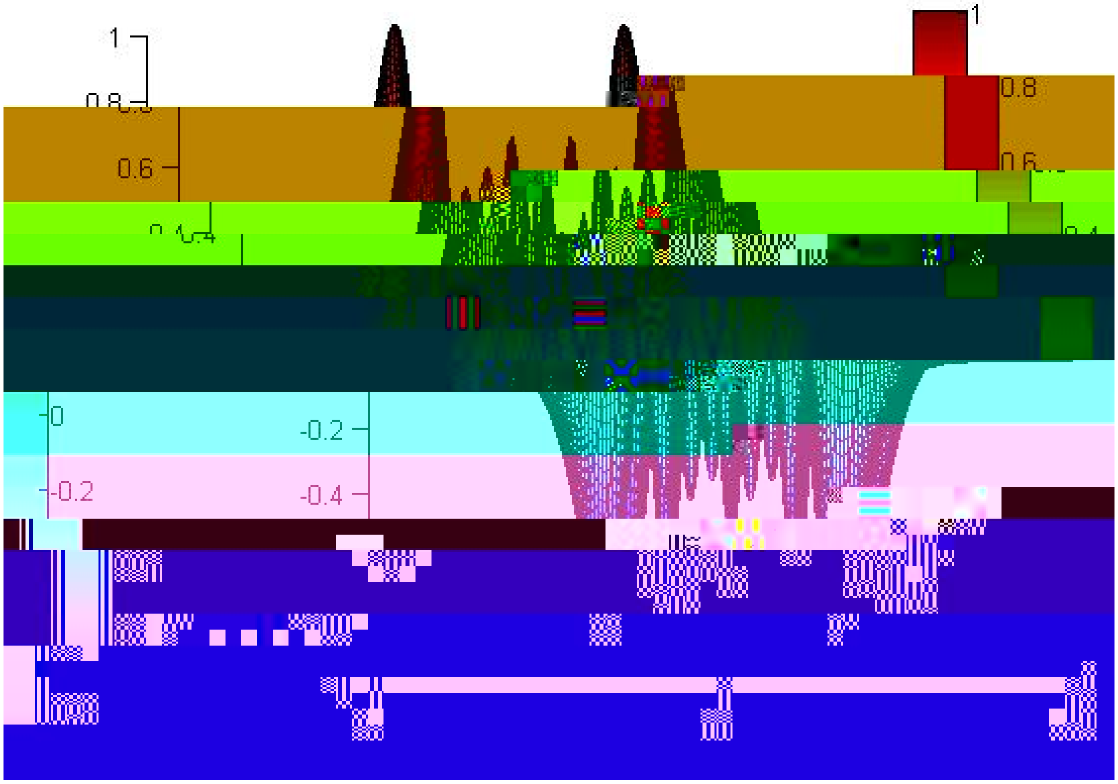

Figure 10: Surface plot of the symmetric trapped modes, where we let $h_1 = 1{:}224$ and wavenumber $k = 1{:}479089$

would expect.

bulge anti-symmetric n=2.jpg

Figure 11: Contour plot of antisymmetric trapped modes for n=2.

Graphs (11) and (12) depict solutions of trapped modes for n=2. Both graphs illustrate the existence of two trapped modes, which we would expect, since by increasing n we are increasing the range of k and the number of Airy solutions available. Therefore we can deduce, increasing n leads to an increase in the number of possible trapped that could exist.

bulge symmetric n=2.jpg

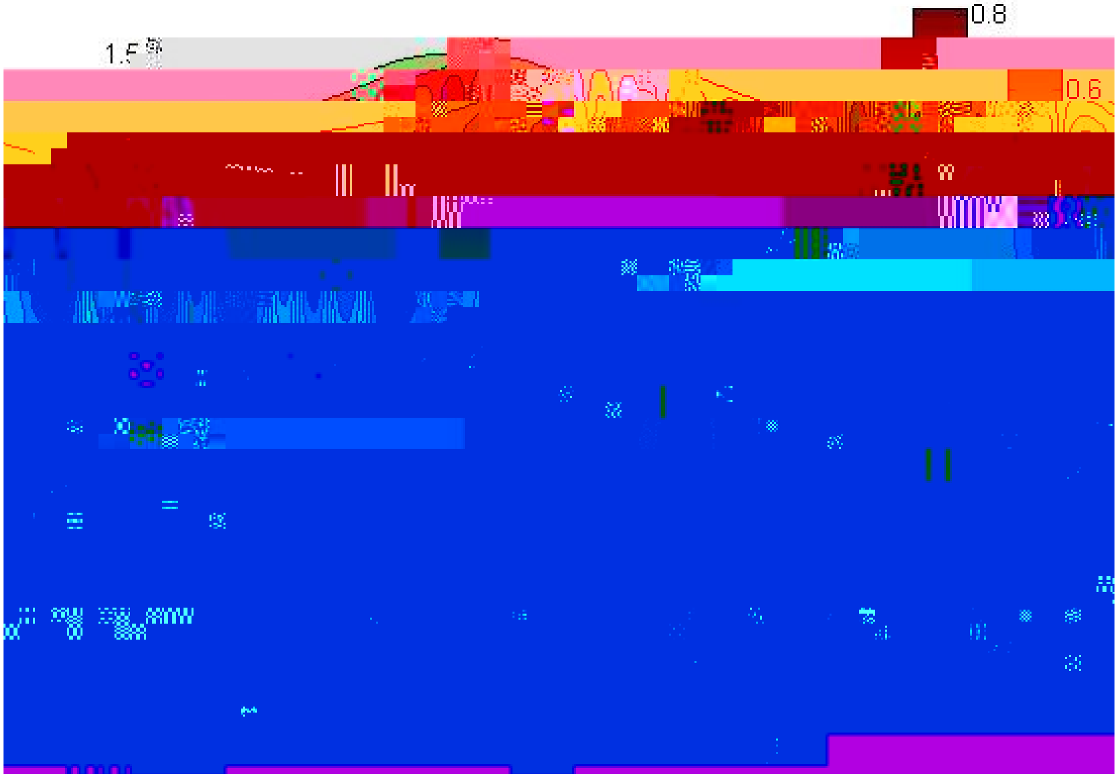

Figure 12: Contour plot of symmetric trapped modes for n=2.

4.3 Plotting the nal solutions with Neumann boundary conditions

We will now compare these trappings with the symmetric and antisymmetric solutions of the Neumann boundary condition. Figures (13) and (14) illustrate resonance occuring at the surface boundary of the bulge region of the duct, unlike the Diriclet case, in which resonance occured in the whole region of the bulging duct. A better look at this di erence, is to analyse the surface plots as illustrated in gures (15) and (16). From these graphs we can see the Neumann boundary conditions, suggest two resonating waves on each side of the boundary. We denoted in earlier chapers h to be the upper and lower boundaries of the duct (see gure

Neumann bulge anti-symmetric n=1.jpg

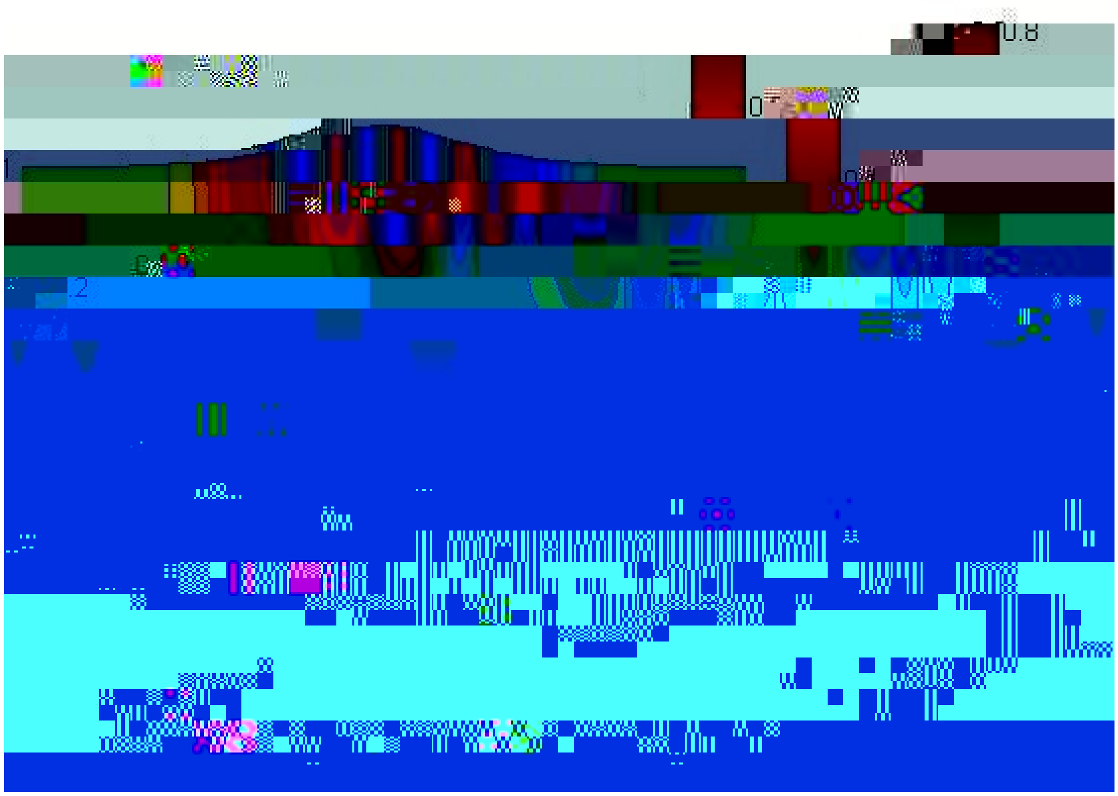

Figure 13: Contour plot of antisymmetric trapped modes, with Neumann boundary condition.

Neumann bulge symmetric n=1.jpg

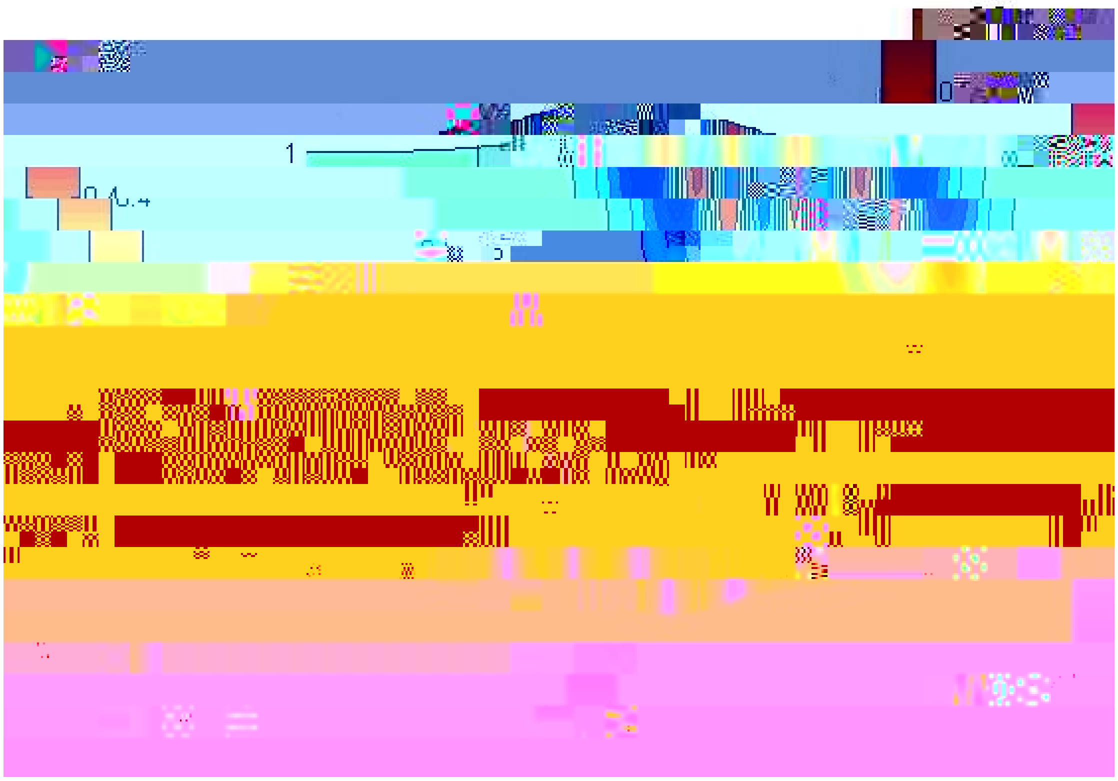

Figure 14: Contour plot of the symmetric trapped modes, with Neumann boundary condition for n = 1.

antisymmetric Neumann.jpg

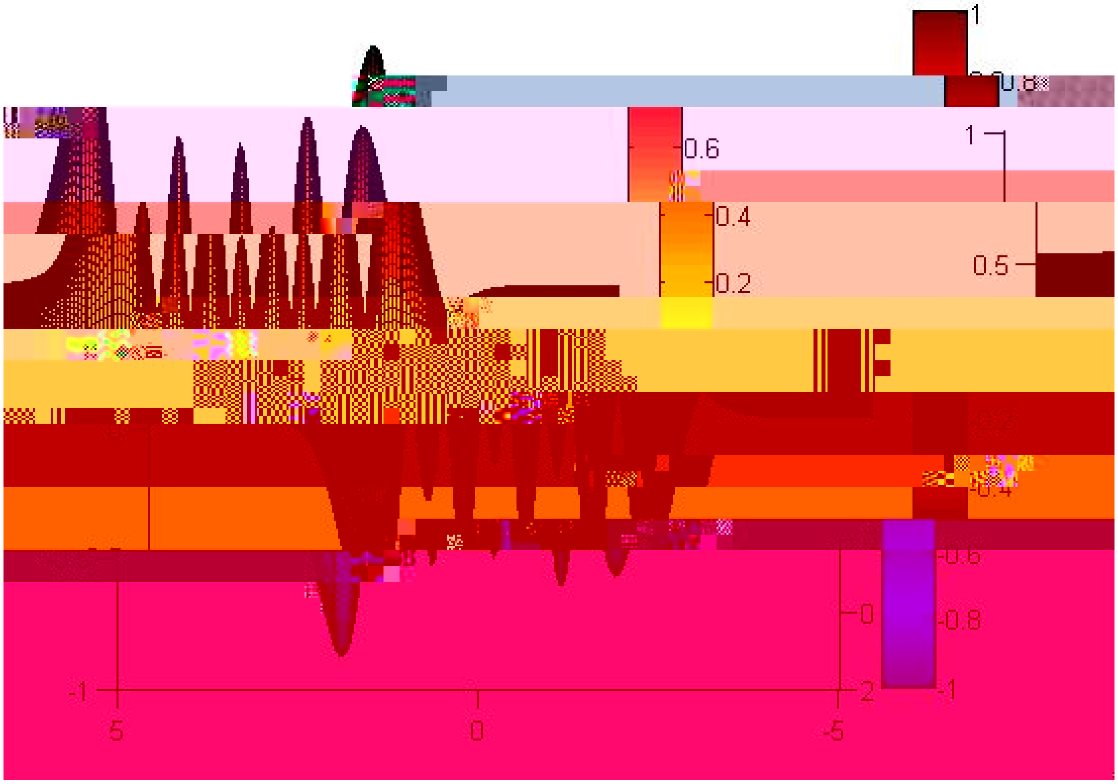

Figure 15: Surface plot of antisymmetric trapped modes, with Neumann boundary condition for n = 1, where we let h_1 = 1:224 and wavenumber k = 1:500052

symmetric Neumann.jpg

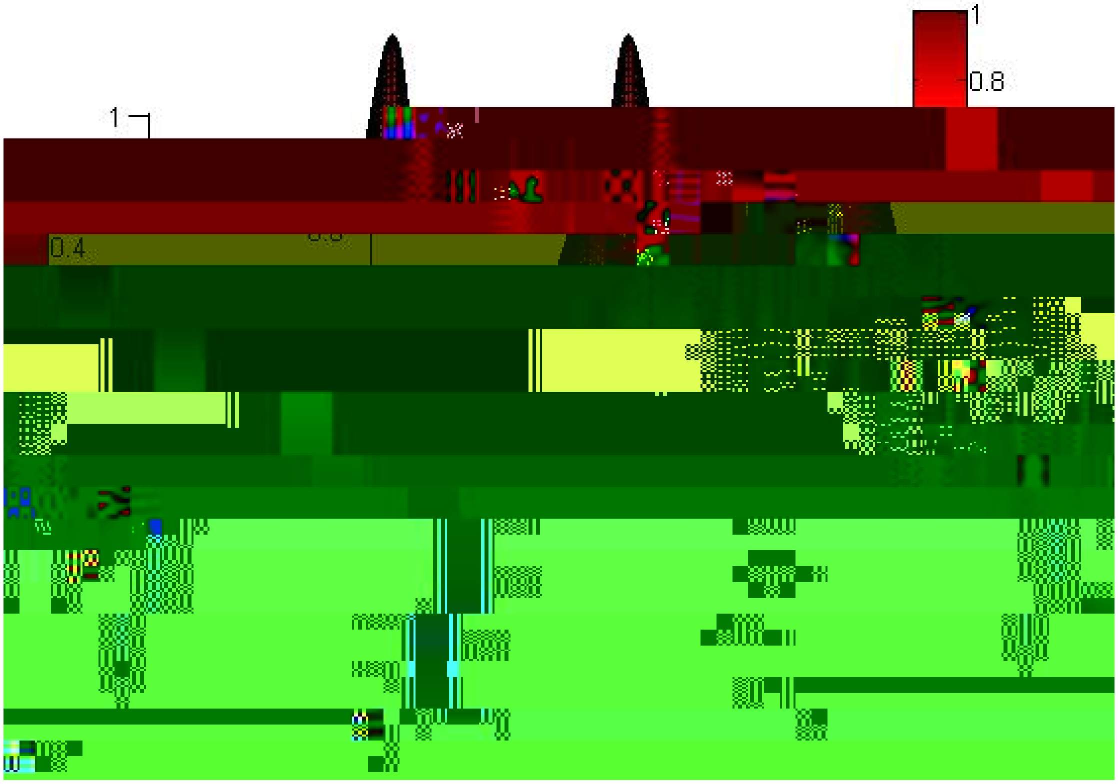

Figure 16: Surface plot of the symmetric trapped modes, with Neumann boundary condition for n=1, where we let $h_1 = 1:224$ and wavenumber $k = 1:479089$

Neumann bulge anti-symmetric n=2.jpg

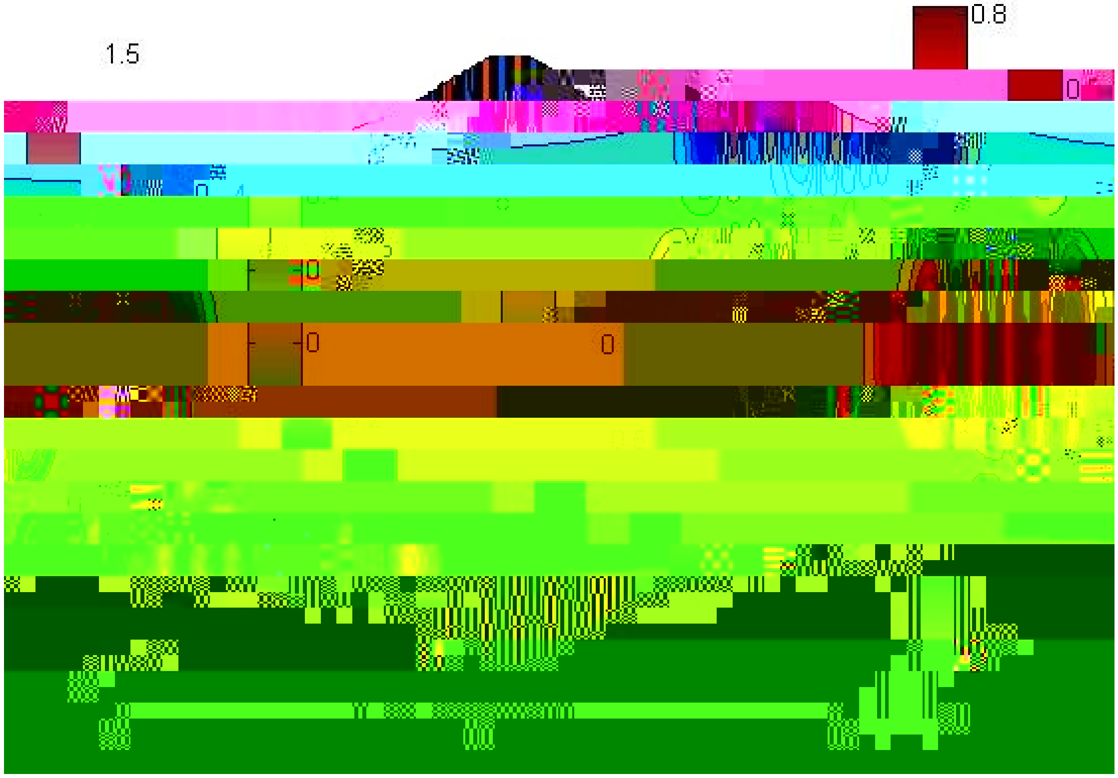

Figure 17: Contour plot of antisymmetric trapped modes, with Neumann boundary condition for n=2.

case again, is very similar to the Dirichlet case, with the main di erence solutions now have three sets of propagating waves. Two occuring on the boundary, and one at the centre. We can deduce that as *n*

Neumann bulge symmetric n=2.jpg

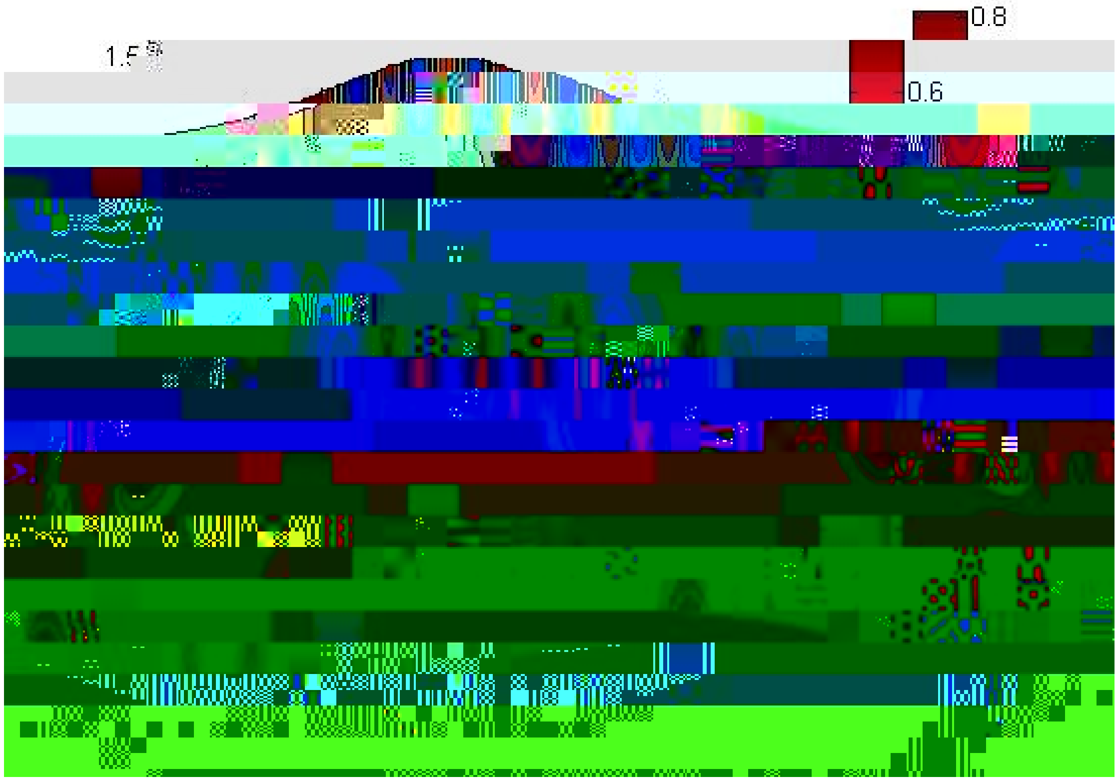

Figure 18: Contour plot of the symmetric trapped modes, with Neumann boundary condition for n=2.

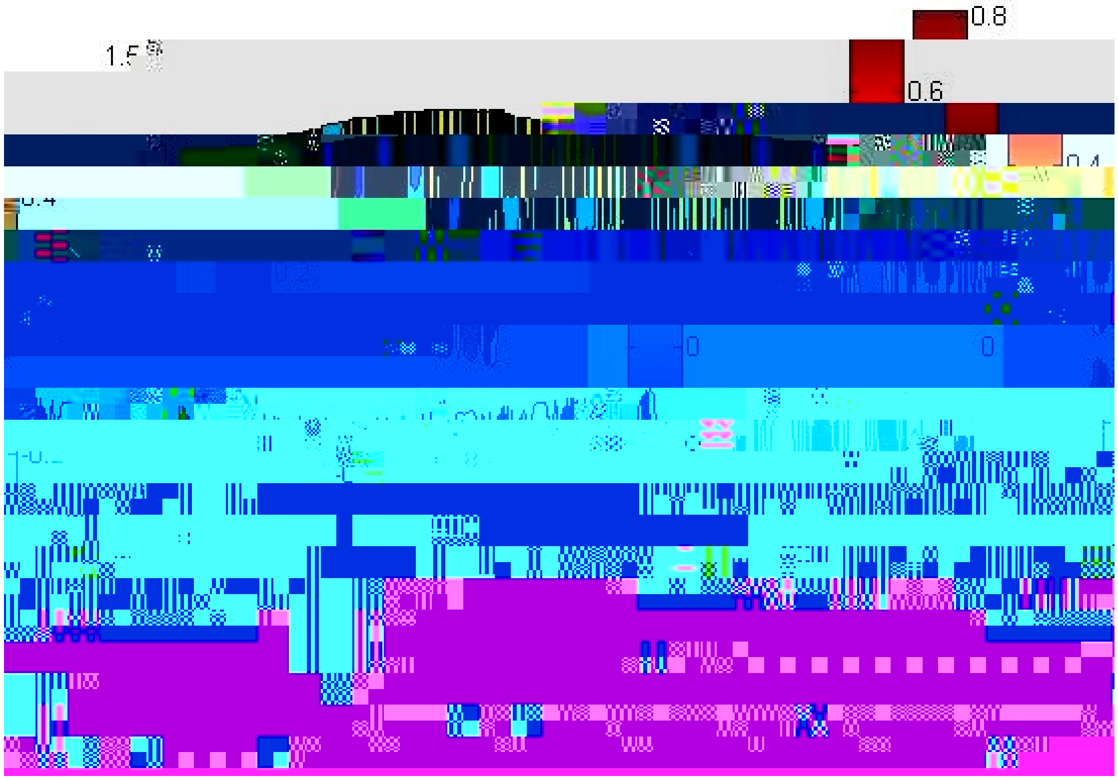

Figure 19: Contour plot of antisymmetric modes, with Neumann condition for $\epsilon = 0.001$.

4.4 Varying the small parameter

Research up until now, on this paper, has dealt with the small parameter $\epsilon = 0.1$, by varying this constant, such that it is even smaller, say 0.001, we find, a rich amount of trappings existing in the region of the bulge. Solutions of the wavenumbers will not be plotted for this paper, as solutions for each Z_n were plotted with marginal gaps between them. As a result, this suggested more trapped modes existed for waveguides, slowly varying as possible. This can be seen from figures (19) and (20) the strong detail in graphs show, many existing trappings occur within the region, and also the affects of the number of oscillations that occur. By letting $\epsilon \to 0$ we increase the number of oscillations within the region. This suggests resonance is greatest for slowly varying waveguides.

Physically this is plausable as it suggest the slower the variation in curvature of the waveguide is the more oscillations can exist.

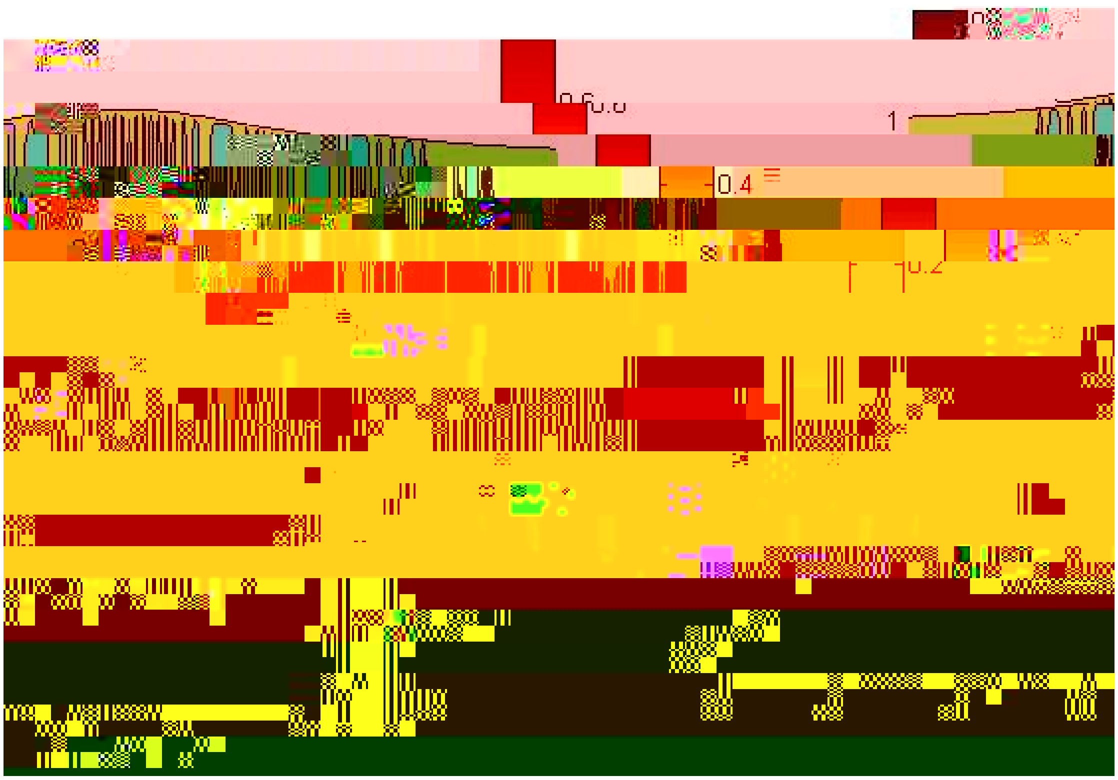

Figure 20: Contour plot of symmetric modes with Dirichlet condition for $\;= 0.001$.

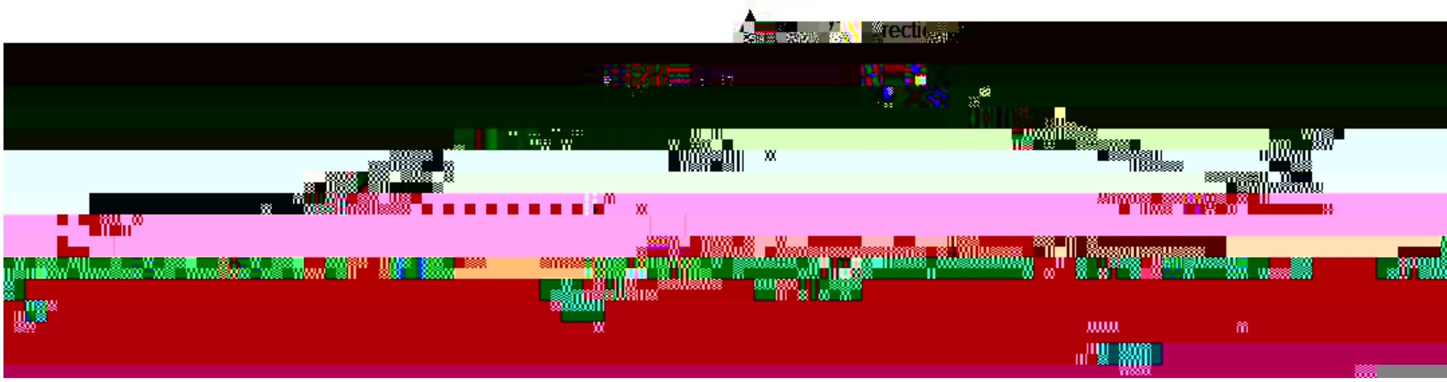

constant n=1 anti-symmetric.jpg

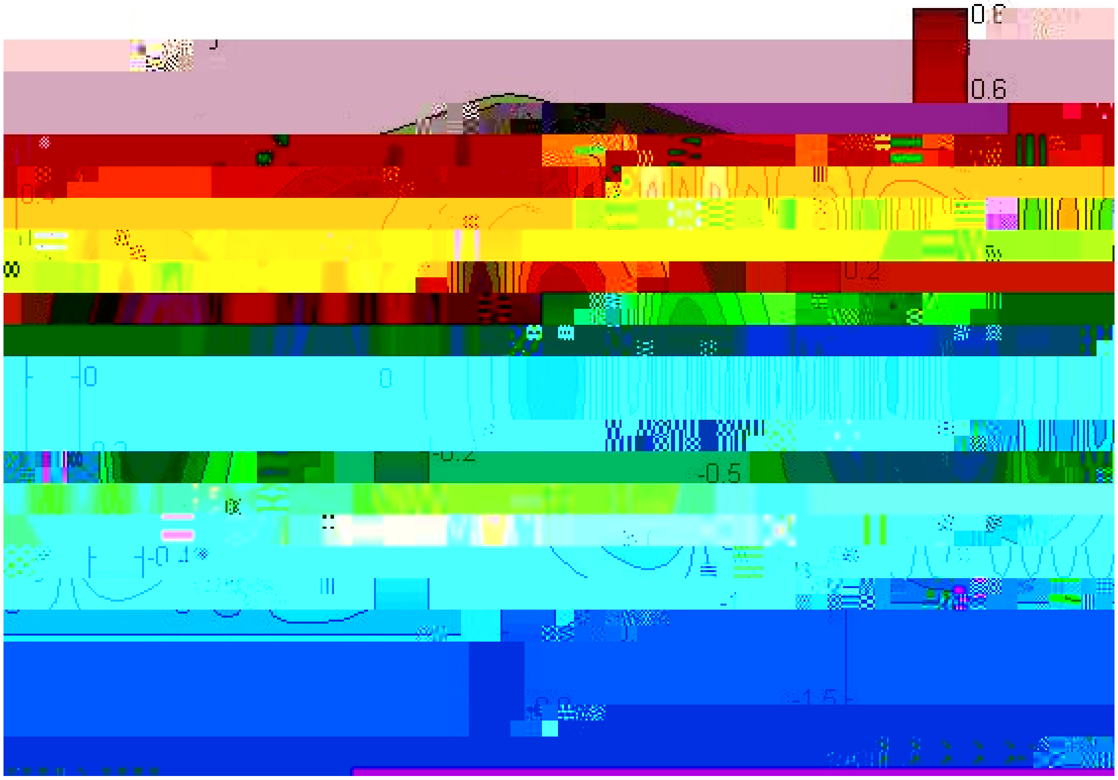

Figure 22: Contour plot of antisymmetric modes, with Dirichlet condition for the new geometrical structure.

constant n=1 symmetric.jpg

Figure 23: Contour plot of symmetric modes with Dirichlet condition for the new geometrical structure.

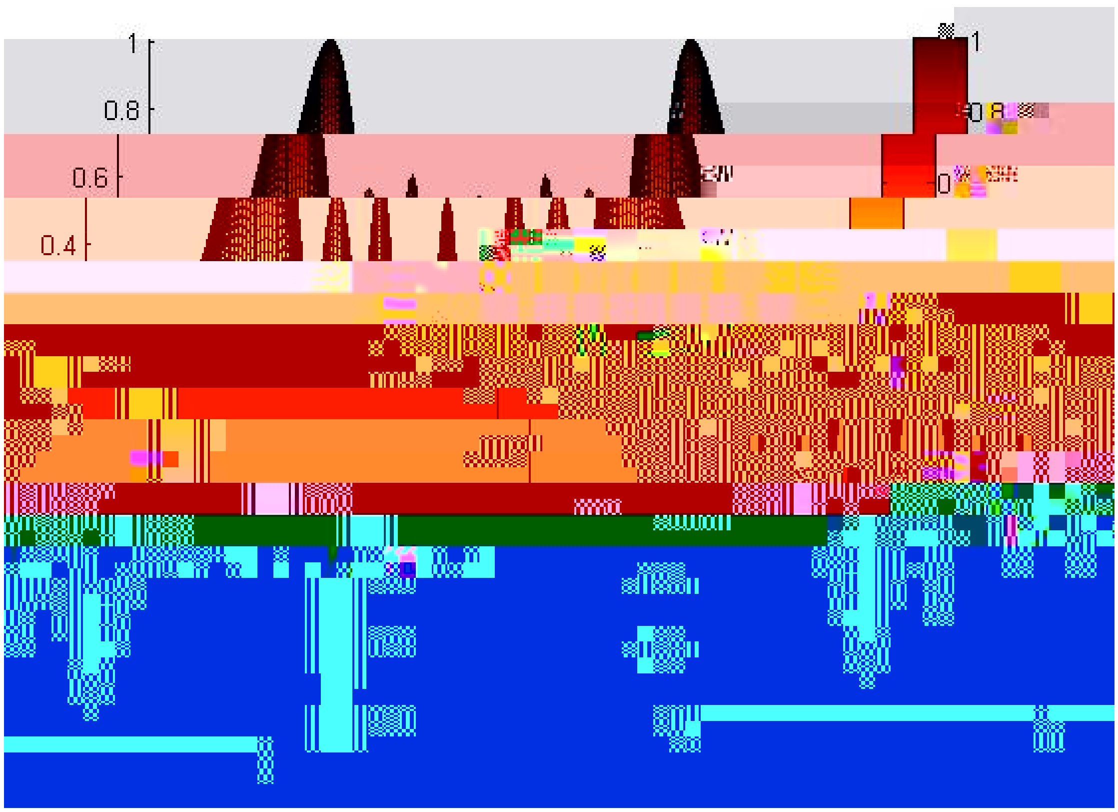

Figure 24: Surface plot of symmetric modes with Dirichlet condition for the new geometrical structure, where h = 1:3012 and k = 1:54682

constant n=2 anti-symmetric.jpg

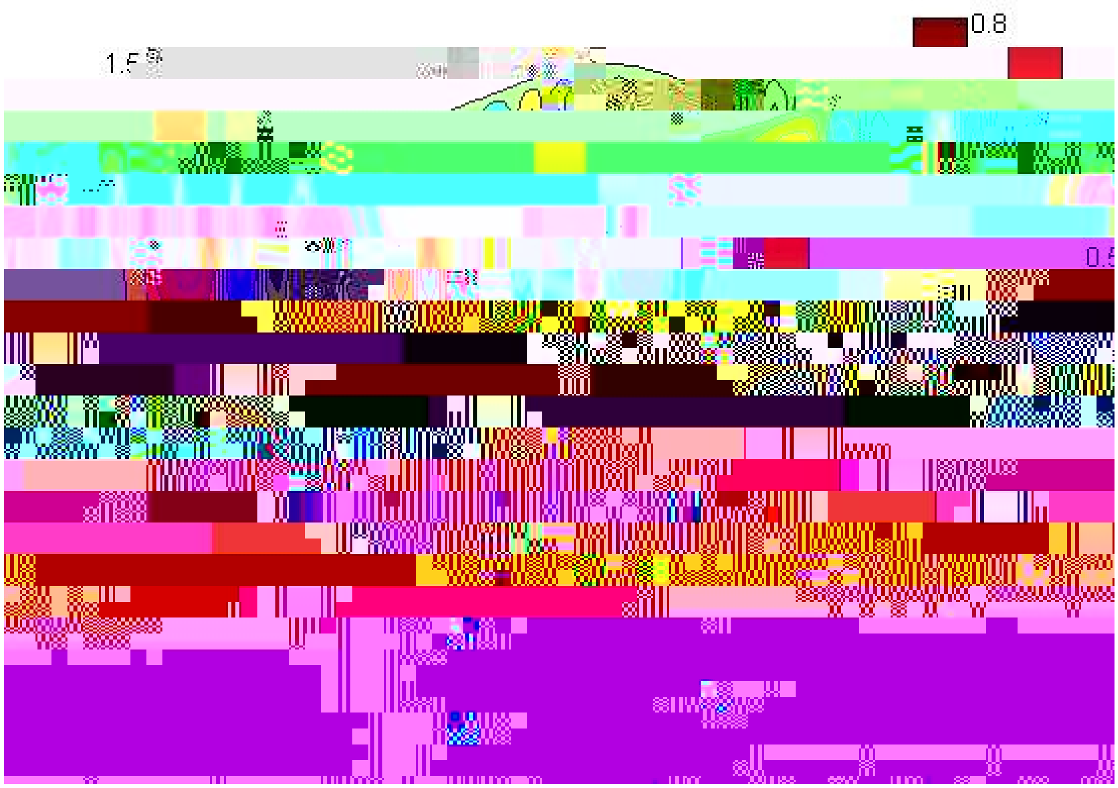

Figure 25: Contour plot of antisymmetric modes, with Dirichlet condition for the new geometrical structure, when $n = 2$.

constant n=2 symmetric.jpg

Figure 26: Contour plot of symmetric modes with Dirichlet condition for the new geometrical structure, when $n = 2$.

Neumann constant anti-symmetric n=1.jpg

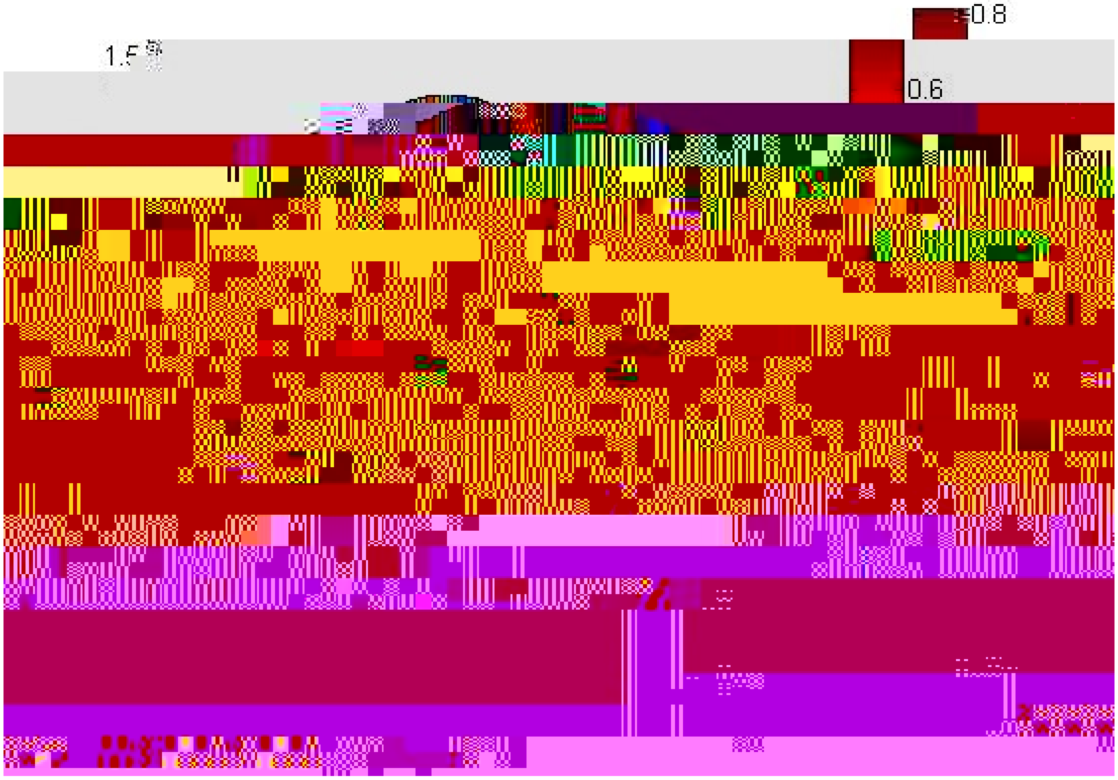

Figure 0 6Td [0 15f

5 Conclusion

In this paper, we have shown trapped modes exist, for slowly varying waveguides of two di erent boundary conditions. Using an asymptotic expansion, we were able to solve the problem for various cases and identify the impact certain physical characteristics have on the solution. In particular, taking

6 First Appendix

List of Airy solutions and the rst derivative solutions			
Z_1	2:338107410459764	Z_1^0	1:018792971647472
Z_2	4:087949444130973	Z_2^0	3:248197582179841
Z_3	5:520559828095556	Z_3^0	4:820099211178738
Z_4	6:786708090071763	Z_4^0	6:163307355639495
Z_5	7:944133587120851	Z_5^0	7:372177255047778
Z_6	9:022650853340979	Z_6^0	8:488486734019723
Z_7	10:040174341558082	Z_7^0	9:535449052433547
Z_8	11:008524303733266	Z_8^0	10:527660396957408
Z_9	11:936015563236262	Z_9^0	11:475056633480246
Z_{10}	12:828776752865757	Z_{10}^0	12:384788371845749
Z_{11}	13:691489035210719	Z_{11}^0	13:262218961665209
Z_{12}	14:527829951775335	Z_{12}^0	14:111501970462996
Z_{13}			

7 Bibliography

This paper is largely based on the works made by Dr. Nick Biggs using the paper of the same name.

References

[1] N.Biggs,\Wave re ection and trapping in a two-dimensional duct,"

[2] J.Postnova, R.V Craster,\Trapped modes in topographically varying elastic waveguides," Wave Motion 44 (2007) 205-221

[3] J.Postnova, R.V Craster,\Trapped modes in elastic plates, oceans and quantum waveguides," Wave Motion 45 (2008) 565-579

[4] A.T.I. Adamou, D. Gridin, R.V Craster,`Acoustic quasi-modes in slowly varying